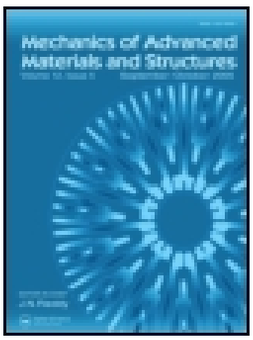

Mechanics of Advanced Materials and Structures

ISSN: 1537-6494 (Print) 1537-6532 (Online) Journal homepage: http://www.tandfonline.com/loi/umcm20

One dimensional nonlocal integro differential model & gradient elasticity model : Approximate solutions and size effects

B. Umesh, A. Rajagopal & J. N. Reddy

To cite this article: B. Umesh, A. Rajagopal & J. N. Reddy (2017): One dimensional nonlocal integro differential model & gradient elasticity model : Approximate solutions and size effects, Mechanics of Advanced Materials and Structures, DOI: 10.1080/15376494.2017.1373313

To link to this article: http://dx.doi.org/10.1080/15376494.2017.1373313

One dimensional nonlocal integro differential model & gradient elasticity model : Approximate solutions and size effects

B. Umesh[a], A. Rajagopal[a] and J. N. Reddy [b]

[a] Dept. of Civil Engg., IIT Hyderabad, Telangana, India
[b] Dept. of Mechanical Engg., Texas A&M University,Texas, USA.

1 Abstract

In the present work, the close similarity that exists between Mindlins strain gradient elasticity and Eringens nonlocal Integro differential model is explored. The methods are studied for one-dimensional examples. Through the proposed approach a relation between length scales of nonlocal-differential and gradient elasticity model is arrived. Further, a relation has also been arrived between the standard and non-standard boundary conditions in both the cases. C^0 based finite element methods are extensively used for the implementation of integro-differential equations. This results in standard diagonally dominant global stiffness matrix with off diagonal elements occupied largely by the kernel values evaluated at various locations. The global stiffness matrix is enriched in this process by nonzero off diagonal terms and helps in incorporation of the nonlocal effect, there by accounting the long range interactions. In this case the diagonally dominant stiffness matrix has a band width equal to influence domain of basis function. In such cases, a very fine discretization with larger number of degrees of freedom are required to predict nonlocal effect, thereby making it computationally expensive.

In the numerical examples, both nonlocal-differential and gradient elasticity model are considered to predict the size effect of tensile bar example. The solutions to integro-differential equations obtained by using various higher order approximations are compared. Lagrangian, Bèzier and B-Spline approximations are considered for the analysis. It has been shown that such higher order approximations have higher inter-element continuity there

by increasing the band width and the nonlocal character of the stiffness matrix. The effect of considering the higher-order and higher-continuous approximation on computational effort is made. In conclusion both the models predict size effect for one-dimensional example. Further, the higher-continuous approximation results in less computational effort for nonlocal-differential model.
Keyword: Eringen nonlocal model, Integro-differential equation, nonlocal-differential model, Kernel function, Mindlin Gradient elasticity models, length scale.

2 Introduction

The classical continuum theory is based on the assumption that the stress defined at a given point is related to strain at the same point. The limitations in continuum theories arise from the facts that, no material is ideal continuum, ignorance of micro-structural details at various length scales and lastly in not accounting the effect of long range interactions. Moreover, there exist certain class of problems at macro-scale, like: strain localization in strain softening material, crack propagation in fracture mechanics, edge effects, stress/strain singularity etc., which all cannot be explained using continuum theories and need the description of material behavior at various scales. The generalized continuum theories introduced to account for the demerits of continuum theories are: couple stress elasticity [1], Theory of elasticity with micro-structure [2], micro-polar and micro-morphic theories [3], multi-polar theory [4, 5] and strain gradient theories [6, 7]. These theories are the mathematical extension of Cosserat continuum theories [8].

The other class of generalized continuum theories that are of interest are the nonlocal theories. The fundamental works on nonlocal theory are made in the late sixties by [9, 10, 11]. Wherein the inability of local theory to handle singularity problems are overcome through nonlocal approach. The main idea is to evaluate stress at a point by accounting strain at all points in the domain. In later days Eringen and co-workers did extensive studies on nonlocal theory and simplified the theory to propose nonlocal constitutive model, wherein the elastic moduli is generalized in order to account the nonlocal effect, see [12, 13, 14, 15]. The work was further extended by Eringen [16] by deriving the differential form of the integro-differential equation. Later, Eringen [17] accounted both local and nonlocal constitutive relation through local-nonlocal constitutive parameter to propose two phase constitutive model. Such advancements in nonlocal theory enabled the researchers to explore the capabilities of nonlocal model in fields of fracture mechanics (see [18, 19]), plasticity (see [20, 21, 22, 23]) and also in damage mechanics (see [24, 25, 26]). At the same time, there where other issues associated with the existence and uniqueness of nonlocal solution for boundary value

problems. In this regard, a strong mathematical basis is derived for the numerical studies of nonlocal elasticity for instance see [27, 28, 29, 30] for details.
Recently, the capability of nonlocal elasticity theory is further explored in predicting size effect of nano-materials. In this context, various beam theories (e.g., Euler-Bernoulli, Timoshenko, Reddy, and Levinson beam theories) were reformulated using Eringen's nonlocal differential constitutive model by Reddy [31], and analytical solutions for bending, buckling, and natural vibrations were also presented. Further, various shear deformation beam theories were also reformulated by Reddy [31]. Nonlocal elastic rod models have been developed to investigate the small-scale effect on axial vibrations of the nano-rods, see [32, 33, 34]. Pisano and Fuschi [35] obtained closed form solution for a nonlocal elastic bar by considering two-phase constitutive model. Benvenuti [36] also made analytical study on nonlocal elastic bar by considering the effect of both material length scale and local-nonlocal parameter. In summary, the size effect is predicted for local parameter greater than one with the condition that the nonlocal solution behaves stiffer than the local solution. Earlier works on generalized continuum theories were proposed by Cosserat et. al. [8]. The simplification and physical understanding of Cosserat theories gave rise to various higher order theories. The difficulty associated with such theories is that the equations are complex together with large number of unknown elastic coefficients. Which made it difficult and inconvenien to experimentalists and designers to account for them precisely [37]. Moreover, these theories are mainly concerned with wave propagation problem and excluding the material instability effects. Motivated from the studies of discrete dislocation dynamics (DDD) in describing the plastic deformation [38, 39], Aifantis introduced gradient plasticity formulation [40, 41, 42] in ascertaining the details of shear band. Fleck et. al. [43] and Gao et. al. [44] proposed strain gradient plasticity based dislocation theory to measure the size-dependent hardness measurement at the micro- and nano-scales. Following the success of gradient plasticity theories, Aifantis [41, 45] proposed simple gradient elasticity model by accounting the Laplacian of strain in the constitutive relations. The model is the special case of the Mindlin gradient elasticity model. Ru and Aifantis [46] further simplified the model by reducing the fourth order equilibrium equation to two set of second order equation. On the other side, Eringen [21] also proposed gradient elasticity model by reformulating the integral type of nonlocal elasticity. A mathematical comparison of both Eringen and Aifantis gradient elasticity model is given in [37]. In summary, Aifantis model is treated as uncoupled model and Eringen model as coupled model. Recently, Rajagopal and Srinivasa [47] proposed an implicit constitutive equation. Which covers various strain gradient elasticity models that appeared in literature. Even though the physics involved in deriving the nonlocal-differential and gradient elasticity models are different, but they share some commonality for certain class of problems. In this regard, very recently Benvenuti and Simone [36] carried out mathematical comparison of both nonlocal-differential and gradient elasticity model by considering one-dimensional

boundary value problem. The work is further extended by Malagaù [48] by exploring the numerical comparison of both nonlocal-differential and gradient elasticity models for nano scaled structural problems. Further, the effect of higher-order approximation in terms of computational efforts is also made. There is also growing interest in research community to explore the close similarities between the nonlocal-differential and gradient elasticity model. Moreover, use of C^0 based finite element approximations in effective modeling of nano scaled problems prove to be computationally expensive [48].
In present work we explore the similarity between the Eringen nonlocal-differential and gradient-elasticity model. A one-dimensional model is considered for the present work. There are issues associated with Mindlins gradient-elasticity model, with regards to experimental measure of (i) higher derivative of displacement field related to non-standard boundary conditions and (ii) specification of material length scale. In present work, such issues are addressed by comparing the both models. Further, the computation efforts are also explored by considering higher order approximation and higher continuity approximation. The paper is organized as follows: The various approximations considered in the present work are discussed in detail in section 3. The higher-continuity approximation is achieved through the B-spline approximation. In section 4 we review the mathematical formulations of Eringen nonlocal model and present in detail the derivation of nonlocal-differential model. The simplified version of Mindlin gradient-elasticity model is reviewed in section 5. Further, a comparison of both the models in terms of boundary conditions and length-scales are made. Galerkin based weighted residual approach is made use to derive the matrix-vector equation in both the cases, see Section 6. The results on one-dimensional numerical examples are presented in last section.

3 Approximation

In numerical approaches the primary variable (displacement) is approximated as a linear combination of basis functions and coefficients. The basis functions are generally kinematically admissible functions of polynomial type. A C^0 continuous based basis polynomials, i.e. Lagrange basis, are the most popular one. Bèzier basis are almost identical to Lagrangian basis, but basis do not interpolate the interior control points. B-spline basis are the generalization of Bèzier basis and have higher order continuity at the inter element boundary. In the following section Lagrangian, Bèzier and B-spline basis functions are explained in detail. The rational form of Bèzier and B-spline basis are also discussed.

3.1 Lagrange polynomial

Given $n+1$ data points, i.e. $(x_0,\, f_0)$, $(x_1,\, f_1)$, ...$(x_j,\, f_j)$, ...$(x_n,\, f_n)$, such that subsequent points are not repeated, then an p^{th} degree Lagrange polynomial is constructed as a linear combination of Lagrange basis polynomials.

$$L(x) \;=\; \sum_{j=0}^{n} f_j\, \ell_j(x) \tag{1}$$

Where Lagrange basis polynomials are obtained as

$$\ell_j(x) = \prod_{\substack{i=0 \\ i\neq j}}^{n} \frac{(x \;-\; x_i)}{(x_j \;-\; x_i)} \tag{2}$$

with the following Kronecker delta property

$$\ell_j(x_k) = \prod_{\substack{i=0 \\ i\neq j}}^{n} \frac{(x_k \;-\; x_i)}{(x_j \;-\; x_i)} = \delta_{jk} = \begin{cases} 1, & if \quad k = j \\ 0, & if \quad k \neq j \end{cases} \tag{3}$$

which makes sure that the polynomial, $L(x_k)$, interpolates all the data points

$$L(x_k) = \sum_{j=0}^{n} f_j \ell_j(x_k) = \sum_{j=0}^{n} f_j \delta_{jk} = f_k \tag{4}$$

A Lagrange basis polynomial plotted for degree 1, 2 and 3 is as shown in Fig. **??**. The derivatives of Lagrange basis polynomials are obtained as follows

$$\ell_j'(x) = \prod_{\substack{i=0 \\ i\neq j}}^{n} \frac{1}{(x_j \;-\; x_m)} \sum_{\substack{i=0 \\ i\neq j}}^{n} \prod_{\substack{k=0 \\ k\neq i \\ k\neq j}}^{n} (x \;-\; x_k) \tag{5}$$

3.2 Bèzier and B-spline polynomial

Given $n+1$ control points, i.e. $\mathrm{P}_0, \mathrm{P}_1, ..., \mathrm{P}_j, ..., \mathrm{P}_n$, an p^{th} degree Bèzier polynomial is constructed as weighted average of all control points

$$\mathrm{P}(\boldsymbol{x}) = \sum_{j=0}^{n} b_j^p(\xi)\, \mathrm{P}_j \tag{6}$$

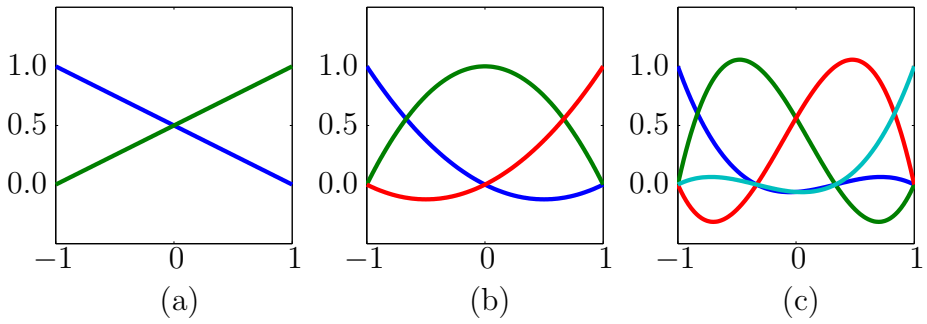

Figure 1: Lagrange basis polynomial: (a) Linear (b) Quadratic (c) Cubic

Where, $b_j^p(\xi)$ are the Bernstein basis polynomials defined as

$$b_j^p(\xi) = \frac{p!}{j!\,(p-j)!}\,(1-\xi)^{p-j}\,\xi^p \tag{7}$$

There exists another technique to obtain higher order Bernstein basis polynomial as a combination of lower order Bernstein basis, and is termed as recursive technique [49]

$$b_j^p(\xi) = (1-\xi)\,b_j^{p-1}(\xi) \;+\; \xi\,b_{j+1}^{p-1}(\xi) \tag{8}$$

Such techniques are useful in describing the derivatives of Bernstein polynomial and also in describing the B-spline basis polynomials, which will be discussed next

$$b_j^{p'}(\xi) = p\,\left\{\, b_{j-1}^{p-1}(\xi) - b_j^{p-1}(\xi)\,\right\} \tag{9}$$

Let $\boldsymbol{K}$ be a vector containing a non-descending sequence in a parameter space, which are defined as

$$\begin{aligned} \boldsymbol{K} &= \{\xi_1, \xi_2, ..., \xi_{n_k}\}, \qquad \xi_i \in \mathbb{R} \\ \text{such that} \qquad & \xi_i \geqslant \xi_{i-1}, \qquad i = 2, 3, ..., n_k \end{aligned} \tag{10}$$

The vector $\boldsymbol{K}$ and scalar ξ_i are often termed as *knot vector* and *knots*, respectively, in computational geometry. Once we define the knot vector, the B-spline basis $N_i^p(\xi)$ of degree

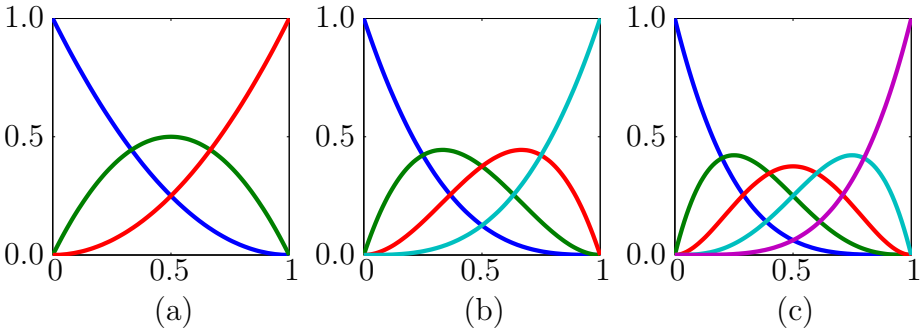

Figure 2: Bèzier basis polynomial: (a) Quadratic (b) Cubic (c) Quintic

$p > 0$ are computed from constant basis using the recursive technique

$$\text{for } p = 0; \quad N_i^0(\xi) = \begin{cases} 1 & \text{if } \xi \in [\xi_i, \xi_{i+1}) \\ 0 & \text{otherwise} \end{cases}$$
$$\text{for } p > 0; \quad N_i^p(\xi) = \begin{cases} \frac{(\xi-\xi_i)}{(\xi_{i+p}-\xi_i)} N_i^{p-1}(\xi) + \frac{(\xi_{i+p+1}-\xi)}{(\xi_{i+p+1}-\xi_{i+1})} N_{i+1}^{p-1}(\xi) & \text{if } \xi \in [\xi_i, \xi_{i+p+1}) \\ 0 & \text{otherwise} \end{cases} \tag{11}$$

The B-spline basis obtained for an arbitrary knot vector are non-interpolatory in nature. In order to get interpolatory form, knots are required to be repeated, which is referred to as the knot multiplicity. In this regard, we introduce an open knot vector containing end knot with knot multiplicity equal to $p+1$. Further, B-spline basis includes other important properties such as

- Partition of unity $\sum_{i=1}^{n_{cp}} N_i^p(\xi) = 1 \quad \forall \quad \xi \in [0, 1)$
- Point-wise positive $N_i^p(\xi) \geqslant 0 \quad \forall \quad \xi \in [0, 1)$
- Kronecker delta $N_i^p(\xi_j) = \delta_{ij} \quad \xi_j \in [\xi_i, \xi_{i+p+1})$

  iff the knot multiplicity of ξ_j equal to p

(12)

The standard geometries, such as a circle or ellipse, are best represented through rational form. In this regard, we generalize the B-spline referred as nonuniform rational B-splines

(NURBS). The same rational form is applicable even for Bèzier basis also.

$$\mathrm{R}_i^p(\xi) = \frac{N_i^p(\xi) w_i}{\sum_{j=0}^{n_{cp}} N_j^p(\xi) w_j} \tag{13}$$

where w_i are the weights associated with the control points. Further, the derivative of the B-spline basis are given as

$$\frac{dN_i^p(\xi)}{d\xi} = \begin{cases} \frac{p}{(\xi_{i+p}-\xi_i)} N_i^{p-1}(\xi) - \frac{p}{(\xi_{i+p+1}-\xi_{i+1})} N_{i+1}^{p-1}(\xi) & \text{if} \quad \xi \in [\xi_i, \xi_{i+p+1}) \\ 0 & \text{otherwise} \end{cases} \tag{14}$$

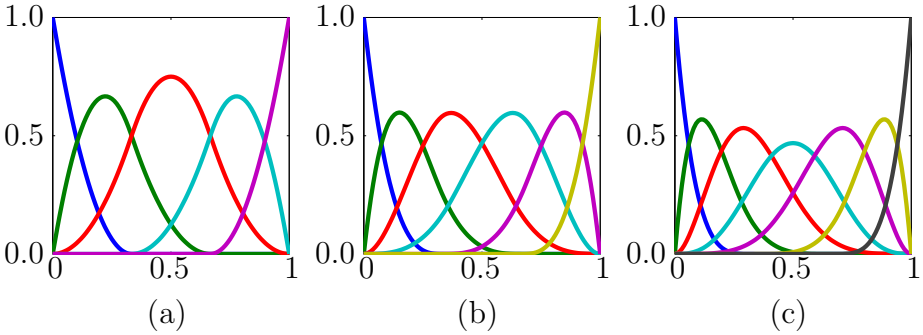

Figure 3: B-spline basis polynomial: (a) Quadratic (b) Cubic (c) Quintic

4 Nonlocal Formulation

Nonlocal theories accounts for long range interactions unlike conventional continuum theories which strongly depends on the concepts of contact forces with zero range. Eringen et. al. [50] simplified nonlocal theories to a great extent and introduced the nonlocal constitutive models, where the generalized elastic stiffness accounts for nonlocal effect. The work is further extended by himself [17] and introduced the nonlocal-differential elasticity model. In the following section the mathematical formulation for the nonlocal constitutive model and nonlocal-differential elasticity model will be explored in detail.

4.1 Nonlocal constitutive model

Consider a material body occupying a geometrical region in real number space, $\Omega \in \mathbb{R}^3$, as shown in Fig. **??**. The surface boundary of the geometrical region is denoted by Γ. Let $\boldsymbol{X}$ be material position vector of material particle, measured from fixed rectangular coordinate system. The spatial position vector measured in same frame is $\boldsymbol{x}$. Then, the infinitesimal displacement vector $\boldsymbol{u}$ to relate the material and spatial position vector can written as

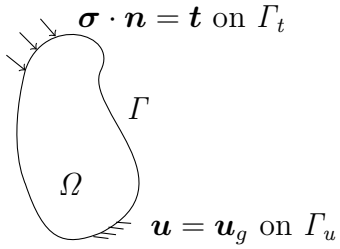

Figure 4: 2D elastic body under consideration

$$\boldsymbol{u}(\boldsymbol{x}) \;=\; \boldsymbol{x} \;-\; \boldsymbol{X} \tag{15}$$

The linearized form of Green-Lagrange strain tensor is written as symmetric part of the displacement gradient termed as infinitesimal strain tensor

$$\boldsymbol{\epsilon}(\boldsymbol{x}) \;=\; \frac{1}{2}\left[\, \boldsymbol{\nabla u} + (\boldsymbol{\nabla u})^T \,\right] \tag{16}$$

Linear elastic theories are based on assumption that the stress at a point is related to the strain at that point through generalized Hooke's law given by, see [51]

$$\boldsymbol{\sigma}(\boldsymbol{x}) = \boldsymbol{C} : \boldsymbol{\epsilon}(\boldsymbol{x}) \tag{17}$$

Where $\boldsymbol{C}$ is fourth order linear elasticity tensor. Whereas in nonlocal theories, Eringen proposed the nonlocal constitutive model as, see [50]

$$\boldsymbol{\sigma}(\boldsymbol{x}) = \int_{\mathrm{V}'} \boldsymbol{C}(\boldsymbol{x}, \boldsymbol{x}', \ell_c) \;:\; \boldsymbol{\epsilon}(\boldsymbol{x}')\, d\mathrm{V}' \tag{18}$$

Where $\boldsymbol{C}(\boldsymbol{x}, \boldsymbol{x}', \ell_c)$ is termed as generalized elastic stiffness. For homogeneous and isotropic material, it is reasonable to replace the generalized elastic stiffness as product of Kernel function and elasticity tensor.

$$\boldsymbol{\sigma}(\boldsymbol{x}) = \int_{\mathrm{V}'} \boldsymbol{C}\, \alpha(\boldsymbol{x}, \boldsymbol{x}', \ell_c) \;:\; \boldsymbol{\epsilon}(\boldsymbol{x}')\, d\mathrm{V}' \tag{19}$$

Where $\alpha(\boldsymbol{x}, \boldsymbol{x}', \ell_c)$ is the Kernel function and ℓ_c material length scale. Further, Kernel function is normalized to result a uniform nonlocal variable for the case of uniform local variable. In the present work an exponential form of Kernel function chosen given by

$$\alpha(\boldsymbol{x}, \boldsymbol{x}', \ell_c) = \frac{1}{2\,\ell_c}\, e^{-|\boldsymbol{x}-\boldsymbol{x}'|/\ell_c} \tag{20}$$

$$\text{such that} \quad \int_{\mathrm{V}'} \alpha(\boldsymbol{x}, \boldsymbol{x}', \ell_c)\, d\mathrm{v}' = 1 \tag{21}$$

In the late 80's, Eringen proposed two phase constitutive relation by weighting both local and nonlocal constitutive model as, see [17]

$$\boldsymbol{\sigma}(\boldsymbol{x}) \;=\; \xi_1\, \boldsymbol{C} \;:\; \boldsymbol{\epsilon}(\boldsymbol{x}) \;+\; \xi_2 \int_{\mathrm{V}'} \alpha(\,\boldsymbol{x},\, \boldsymbol{x}',\, \ell_c\,)\, \boldsymbol{C} \;:\; \boldsymbol{\epsilon}(\boldsymbol{x}')\, d\mathrm{V}' \tag{22}$$

The weights ξ_1 and ξ_2 are termed as local and nonlocal constitutive parameters. A complete local constitutive relation is recovered for the case $\xi_1 = 0$ and $\xi_2 = 1$ and the another possible case is $\xi_1 = 0$ and $\xi_2 = 1$ corresponds to Eringen nonlocal constitutive relation. The equilibrium equation obtained for eq. 22 is termed as integro-differential equation.

4.2 Nonlocal-differential elasticity model

A one-dimensional tensile bar, see fig. **??**, is considered to derive the differential form of integro-differential equation. The geometrical detail includes: L: length of the bar, A: uniform cross sectional area. Let E represents the material elastic modulus. The bar is subjected to load (t) at right end and clamped at left end. The achieved external boundary conditions results in a uniform stress of intensity $\bar{\sigma}$ in the bar. The Eringen nonlocal constitutive model , i.e. eq. 22, can be rewritten as

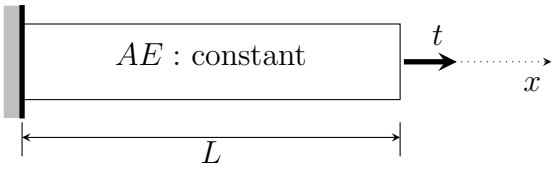

Figure 5: Homogeneous Linear elastic material

$$\sigma(x) \;=\; \xi_1\, E\, \epsilon(x) \;+\; \xi_2\, E\, \epsilon_{nl}(x) \tag{23}$$

Where, the nonlocal strain field is defined as

$$\epsilon_{nl}(x) \;=\; \int_{\mathrm{V}'} \alpha(\, x, x', \ell_c\,)\, \epsilon(x')\, d\mathrm{V}' \tag{24}$$

In the case of tensile bar subjected to concentrated load, i.e. body force equal to zero, the stress at every cross section is equal to $\bar{\sigma}$, i.e. $\sigma(x) = \bar{\sigma}$, by equilibrium. As a result, the eq. 23 is written as

$$\bar{\epsilon} \;=\; \xi_1\, \epsilon(x) \;+\; \xi_2\, \epsilon_{nl}(x) \tag{25}$$

Where, $\bar{\epsilon} \;=\; \bar{\sigma}/E$ uniform strain field. In regard to derive differential form of integro-differential equation, the explicit presence of $\epsilon_{nl}(x)$ in eq. 25 has to be removed. A two step procedure is considered to perform the task: (i) multiply the eq. 25 by $-\ell_c^2 \frac{d^2}{dx^2}$ and (ii) subtract the latest equation from eq. 25.

$$-\ell_c^2\, \frac{d^2\bar{\epsilon}}{dx^2} \;=\; -\ell_c^2\, \xi_1\, \frac{d^2\epsilon(x)}{dx^2} \;-\; \ell_c^2\, \xi_2\, \frac{d^2\epsilon_{nl}(x)}{dx^2} \tag{26}$$

where,

$$\frac{d^2\epsilon_{nl}(x)}{dx^2} = -\frac{1}{\ell_c^2}\epsilon(x) + \frac{1}{\ell_c^2}\epsilon_{nl}(x) \tag{27}$$

Including eq. 27 into eq. 26 results

$$-\ell_c^2\, \frac{d^2\bar{\epsilon}}{dx^2} \;=\; -\ell_c^2\, \xi_1\, \frac{d^2\epsilon(x)}{dx^2} \;+\; \xi_2\epsilon(x) \;-\; \xi_2\, \epsilon_{nl}(x) \tag{28}$$

Subtracting eq. 28 from eq. 25 gives

$$(\xi_1 \;+\; \xi_2)\, \epsilon(x) \;-\; \ell_c^2\, \xi_1 \frac{d^2\epsilon(x)}{dx^2} = \bar{\epsilon} \;-\; \ell_c^2\, \frac{d^2\bar{\epsilon}}{dx^2} \tag{29}$$

The eq. 29 is the differential form in terms of $\epsilon(x)$ for the replacement of eq. 23. The differential form is classified into three category depending upon the type of solution, see [52], and are listed in Table 1. Further, it is suggested to consider $\xi_1 > 0$ to get meaning full solution to the differential form, see [53, 54, 36]

Polianin and Manzhirov [52] obtained analytical solutions for eq. 29. Benvenuti and simone [36] extended the same work for nano scale-problems. The analytical solution obtained predict the size effect correctly following the constraints: (i) The local solution is recovered

Type	$\xi_1 + \xi_2$	solution
01	$= 0$	polynomial
02	< 0	harmonic
03	> 0	exponential

Table 1: Types of differential form

for vanishing length scale and (ii) the nonlocal solution is stiffer than the local one. The first condition is ensured by allowing $\xi_1 + \xi_2 = 1$, see [36]. The nonlocal solution can be made either stiffer or flexible than local solution depending on the value of ξ_1, i.e. $\xi_1 < 1$ corresponds to flexible solution and a stiffer solution is obtained for $\xi_1 > 1$. In the case of flexible solution, the size effect is not predicted correctly for the increasing value of ξ_1, see [35, 36]. Hence, the nonlocal parameter values: $\xi_1 + \xi_2 = 1$ and $\xi_1 \geq 1$, are considered to simplify the eq. 29 , see [52, 53, 54, 36] for more details.

$$E\,\epsilon(x) \;-\; \ell_c^2\,E\,\xi_1 \frac{d^2\epsilon(x)}{dx^2} = \bar{\sigma} \tag{30}$$

The equilibrium equation of one-dimensional problem is given by

$$\frac{d\bar{\sigma}}{dx} = 0 \tag{31}$$

Including eq. 30 into eq. 31 results an higher order differential equation in-terms of displacement

$$E\frac{d}{dx}\left\{\frac{du(x)}{dx}\right\} \;-\; E\,\ell_c^2\,\xi_1\,\frac{d^3}{dx^3}\left\{\frac{du(x)}{dx}\right\} = 0 \tag{32}$$

The boundary conditions derived are as follows, see Appendix 8 for derivation

$$EA\,\ell_c\,\frac{d}{dx}\left\{\frac{du(0)}{dx}\right\} \;-\; EA\,\left\{\frac{du(0)}{dx}\right\} \;=\; -\,\frac{t}{\xi_1} \tag{33}$$

$$EA\,\ell_c\,\frac{d}{dx}\left\{\frac{du(L)}{dx}\right\} \;+\; EA\,\left\{\frac{du(L)}{dx}\right\} \;=\; \frac{t}{\xi_1} \tag{34}$$

A Neumann type of boundary conditions are arrived with eq. 33 referring to constraint (or internal) force at the right end and eq. 34 to external force at the left end of tensile bar.

5 Strain Gradient Elasticity Formulation

In this section, we present the strain gradient elasticity formulation [2]. Wherein, the features of micro-structure is accounted by introducing kinematics at micro-scale, i.e. by considering the micro-deformation and gradient of micro-deformation. The strong form of the Mindlin model is derived by using principle of virtual work. In order to explore the capability of model a simplified version is considered. In regard to implementation the simplified model is derived for one-dimensional case and comparison with Eringen nonlocal-differential elasticity model is made.

5.1 Kinematics at macro- and micro-scale

Consider a material body Ω as shown in Fig. **??**. The surface boundary of the Ω is denoted by Γ. Let $\boldsymbol{X}$ and $\boldsymbol{x}$ be macro and spatial position vector of macro-material particle. Then, the infinitesimal macro-displacement vector and macro-strain tensor is given in eqs. 15 and 16

The classical theories fail to account information available at micro-structure, as the material are not continuous at micro-structure. One of the early attempts includes the work done by Mindlin [2]. Wherein micro-structure features are accounted in deriving three-dimensional linear theory of elasticity. Let us assume that, within each macro-material point there exist a micro-region denoted by Ω'. Further, $\boldsymbol{X}'$ and $\boldsymbol{x}'$ be material and spatial position vector of micro-material particle such that the origin is fixed in the particle. Then, the micro-displacement vector ($\boldsymbol{u}'$) is given by

$$\boldsymbol{u}'(\boldsymbol{x}', \boldsymbol{x}) = \boldsymbol{x}' - \boldsymbol{X}' \tag{35}$$

The explicit depends of micro-displacement with micro-coordinate ($\boldsymbol{x}'$) makes further formulation complex. In this regard, the micro-displacement is approximated accurately as product of functions explicitly depend on $\boldsymbol{x}'$ and $\boldsymbol{x}$ as given below

$$\boldsymbol{u}'(\boldsymbol{x}) = \boldsymbol{x}'\boldsymbol{\psi}(\boldsymbol{x}) \tag{36}$$

Where,

$$\boldsymbol{\psi}(\boldsymbol{x}) = \frac{\partial \boldsymbol{u}'}{\partial \boldsymbol{x}'} \tag{37}$$

is termed as micro-deformation. Further, relative deformation, $\boldsymbol{\gamma}(\boldsymbol{x})$, as difference of macro-displacement gradient and micro-deformation and also a micro-deformation gradient, $\boldsymbol{\kappa}(\boldsymbol{x})$, is given by

$$\boldsymbol{\gamma}(\boldsymbol{x}) = \boldsymbol{\nabla}\boldsymbol{u}(\boldsymbol{x}) - \boldsymbol{\psi}(\boldsymbol{x}) \tag{38}$$

$$\boldsymbol{\kappa}(\boldsymbol{x}) = \boldsymbol{\nabla}\boldsymbol{\psi}(\boldsymbol{x}) \tag{39}$$

5.2 Principle of virtual work

The strain energy density stored by a system in undergoing deformation is given in eq. 40, considering $\boldsymbol{u}$ and $\boldsymbol{\psi}$ as independent variable at macro- and micro-scale. Further, eq. 41 gives the virtual work of internal forces.

$$\mathrm{W} = \mathrm{W}(\,\boldsymbol{\epsilon},\,\boldsymbol{\gamma},\,\boldsymbol{\kappa}\,) \tag{40}$$

$$\delta\mathrm{W} \;=\; \boldsymbol{\tau} \;:\; \delta\boldsymbol{\epsilon} \;+\; \boldsymbol{\alpha} :\; \delta\boldsymbol{\gamma} \;+\; \boldsymbol{\mu} \vdots \delta\boldsymbol{\kappa} \tag{41}$$

Where, $\boldsymbol{\tau}$, $\boldsymbol{\alpha}$ and $\boldsymbol{\mu}$ are Cauchy stress, relative stress and double stress which are the energy conjugate of deformation. Including eq. 38 into eq. 41 results

$$\delta\mathrm{W} \;=\; \boldsymbol{\sigma} \;:\; \boldsymbol{\nabla}\delta\boldsymbol{u} \;-\; \boldsymbol{\alpha} :\; \delta\boldsymbol{\psi} \;+\; \boldsymbol{\mu} \vdots \boldsymbol{\nabla}\delta\boldsymbol{\psi} \tag{42}$$

Where,

$$\boldsymbol{\sigma} = \boldsymbol{\tau} + \boldsymbol{\alpha} \tag{43}$$

is termed as total stress. By making use of rule of differentiation eq. 42 is further simplified as

$$\delta\mathrm{W} \;=\; \boldsymbol{\nabla}\cdot(\,\boldsymbol{\sigma}\cdot\delta\boldsymbol{u}\,) \;-\; (\,\boldsymbol{\nabla}\cdot\boldsymbol{\sigma}\,)\cdot\delta\boldsymbol{u} \;-\; \boldsymbol{\alpha} :\; \delta\boldsymbol{\psi} \;+\; \boldsymbol{\nabla}\cdot(\,\boldsymbol{\mu}\colon\delta\boldsymbol{\psi}\,) \;-\; (\,\boldsymbol{\nabla}\cdot\boldsymbol{\mu}\,)\colon\delta\boldsymbol{\psi} \tag{44}$$

Then, the total strain energy obtained by a system is given by

$$\delta\mathcal{W}^i \;=\; \int_\Omega \delta\mathrm{W}\, d\Omega \tag{45}$$

Including eq. 44 in eq. 45 and also making use of divergence theorem the final form is given in eq.46.

$$\delta\mathcal{W}^i \;=\; -\int_\Omega \{\,(\,\boldsymbol{\nabla}\cdot\boldsymbol{\sigma}\,)\cdot\delta\boldsymbol{u}\,\}\, d\Omega \;-\; \int_\Omega \{\,(\,\boldsymbol{\alpha} \;+\; \boldsymbol{\nabla}\cdot\boldsymbol{\mu}\,)\colon\delta\boldsymbol{\psi}\}\, d\Omega \;+\; \int_\Gamma \boldsymbol{n}\cdot(\,\boldsymbol{\sigma}\cdot\delta\boldsymbol{u}\,)\, d\Gamma \;+\; \int_\Gamma \boldsymbol{n}\cdot(\,\boldsymbol{\mu}\colon\delta\boldsymbol{\psi}\,)\, d\Gamma \tag{46}$$

Let, $\boldsymbol{b}$ and $\boldsymbol{t}$ be the body force per unit volume and surface traction per unit area associated with virtual variable $\delta\boldsymbol{u}$. Similarly, allowing $\boldsymbol{\Phi}$ and $\boldsymbol{T}$ as double force per unit volume and

double force per unit area for virtual variable $\delta\boldsymbol{\psi}$. Then, the virtual work done by the external forces is expressed as

$$\delta\mathcal{W}^e = \int_\Omega \boldsymbol{b}\cdot\delta\boldsymbol{u}\,d\Omega + \int_\Gamma \boldsymbol{t}\cdot\delta\boldsymbol{u}\,d\Gamma + \int_\Omega \boldsymbol{\Phi}\colon\delta\boldsymbol{\psi}\,d\Omega + \int_\Gamma \boldsymbol{T}\colon\delta\boldsymbol{\psi}\,d\Gamma \tag{47}$$

The principle of virtual work states that for given system in equilibrium the total work done by all internal and external forces vanishes for any virtual displacement which is consistent with constraint, i.e.

$$\delta\mathcal{W}^i - \delta\mathcal{W}^e = 0 \tag{48}$$

Including eqs. 46 and 47 into eq. 48 and splitting the equation into macro- and micro-parts results in two equilibrium equation and concerned traction boundary conditions.

$$\boldsymbol{\nabla}\cdot\boldsymbol{\sigma} + \boldsymbol{b} = 0 \tag{49}$$

$$\boldsymbol{\alpha} + \boldsymbol{\nabla}\cdot\boldsymbol{\mu} + \boldsymbol{\Phi} = 0 \tag{50}$$

$$\boldsymbol{\sigma}\cdot\boldsymbol{n} = \boldsymbol{t} \tag{51}$$

$$\boldsymbol{\mu}\cdot\boldsymbol{n} = \boldsymbol{T} \tag{52}$$

In order give more insight into Mindlin higher order theory we restrict theory stating that macro- and micro-deformation coincides which results into the following mathematical relations

$$\boldsymbol{\nabla u} = \boldsymbol{\psi} \tag{53}$$

$$\text{i.e. } \boldsymbol{\gamma} = 0 \;\;\&\;\; \boldsymbol{\kappa} = \boldsymbol{\nabla\epsilon} \tag{54}$$

Wherein, the relative deformation vanishes. Accordingly, the strain energy density becomes explicit function of $\boldsymbol{\epsilon}$ and $\boldsymbol{\nabla\epsilon}$ only

$$\mathrm{W} = \mathrm{W}(\boldsymbol{\epsilon}, \boldsymbol{\nabla\epsilon}) \tag{55}$$

$$\delta\mathrm{W} = \boldsymbol{\sigma}\colon\delta\boldsymbol{\epsilon} + \boldsymbol{\mu}\vdots\boldsymbol{\nabla}\delta\boldsymbol{\epsilon} \tag{56}$$

The total stress becomes equal to the Cauchy stress, i.e. $\boldsymbol{\sigma} = \boldsymbol{\tau}$. Further, we also state that the virtual work done higher order stress, in particular the domain part, is not accounted for simplicity in implementation, i.e. eq. 46 modified as

$$\delta\mathcal{W}^i \;=\; -\int_\Omega \{\,(\,\boldsymbol{\nabla}\cdot\boldsymbol{\sigma}\,)\cdot\delta\boldsymbol{u}\,\}\,d\Omega \;+\; \int_\Gamma \boldsymbol{n}\cdot(\,\boldsymbol{\sigma}\cdot\delta\boldsymbol{u}\,)\,d\Gamma \;+\; \int_\Gamma \boldsymbol{n}\cdot(\,\boldsymbol{\mu}\colon\delta\boldsymbol{\epsilon}\,)\,d\Gamma \tag{57}$$

The virtual work done by external forces remains same as eq. 47 excluding only the double force per unit volume term. Then including the $\delta\mathcal{W}^i$ and $\delta\mathcal{W}^e$ into eq. 48 results into same equilibrium equation, eq. 49 and traction boundary conditions, eqs. 51-52. The simplified Mindlin higher order theory discussed is closely related to the Casal's anisotropic model for linear elasticity, see [55].

5.3 Simplified Mindlin higher order model for one-dimension

A one-dimensional example is considered to demonstrate the simplified version of Mindlin higher order model, see Fig. **??**. The total work done by system due to internal and external forces are given in eq. 58, wherein the contribution of higher order stress is limited to surface boundary integral

$$\mathcal{W} = \frac{1}{2}\int_0^L A\,\sigma(x)\,\epsilon(x)\,dx \;+\; A\,\mu(x)\,\epsilon(x)\Big|_\Gamma \tag{58}$$

Further, the constitutive relation given by Casal's for Cauchy and double stress are assumed in the present work [55]

$$\sigma(x) \;=\; E\,\frac{du(x)}{dx} \;-\; E\ell_c^{g^2}\,\frac{d^2}{dx^2}\left\{\frac{du(x)}{dx}\right\} \tag{59}$$

$$\mu(x) \;=\; E\ell_c^{g^2}\,\frac{d}{dx}\left\{\frac{du(x)}{dx}\right\} \tag{60}$$

Wher, ℓ_c^g is the material length scale associated with gradient theory. Including the eqs. 59-60 into eq. 58 and equating virtual work done by all forces to zero results in following equation.

$$\int_0^L \left[EA\frac{d}{dx}\left\{\frac{du(x)}{dx}\right\} \;-\; EA\ell_c^{g^2}\,\frac{d^3}{dx^3}\left\{\frac{du(x)}{dx}\right\}\right]\delta u(x)\,dx \;-$$

$$\left[EA\left\{\frac{du(x)}{dx}\right\} \;-\; EA\ell_c^{g^2}\,\frac{d^2}{dx^2}\left\{\frac{du(x)}{dx}\right\}\right]\delta u(x)\Big|_\Gamma \;+\; \left[EA\ell_c^{g^2}\,\frac{d}{dx}\left\{\frac{du(x)}{dx}\right\}\right]\frac{d\delta u(x)}{dx}\Big|_\Gamma = 0 \tag{61}$$

Here, treating $\delta u(x)$ and $\frac{d\delta u(x)}{dx}$ as a independent variable. Then, the above equation gives following equilibrium equation, eq. 62, and boundary conditions, eqs 63-66.

$$EA\frac{d}{dx}\left\{\frac{du(x)}{dx}\right\} - EA\ell_c^{g^2}\frac{d^3}{dx^3}\left\{\frac{du(x)}{dx}\right\} = 0 \quad \text{in} \quad (0, L) \tag{62}$$

$$EA\left\{\frac{du(x)}{dx}\right\} - EA\ell_c^{g^2}\frac{d^2}{dx^2}\left\{\frac{du(x)}{dx}\right\} = t \quad \text{on} \quad \Gamma_t \tag{63}$$

$$EA\ell_c^{g^2}\frac{d}{dx}\left\{\frac{du(x)}{dx}\right\} = T \quad \text{on} \quad \Gamma_t^* \tag{64}$$

$$u(x) = u_g \quad \text{on} \quad \Gamma_u \tag{65}$$

$$\frac{du(x)}{dx} = \left(\frac{du}{dx}\right)_g \quad \text{on} \quad \Gamma_u^* \tag{66}$$

Comparing the nonlocal-differential and gradient elasticity model the following remarks are made:

Remark 1. *The constitutive relation derived in both cases, i.e. eqs. 30 and 59, remain same with $\ell_c^g = \ell_c\sqrt{\xi_1}$. The length scale ($\ell_c$) in nonlocal theory accounts for the influence region and magnitude of nonlocal effect. Whereas, the length scale (ℓ_c^g) in strain gradient theory is related to micro-structural dimension. In earlier cases, for continuous material the ℓ_c^g is evaluated by related it to the size of representative volume element (RVE). Later it is observed that for strain softening material the approach becomes meaningless [37]. Further, various advanced experiments are suggested to evaluate ℓ_c^g. But with proposed approaches it is possible to quantify ℓ_c^g through ℓ_c.*

Remark 2. *The equation of motion derived remains identical for both the approaches. Looking carefully into eq. 62 the first term correspond to equation of motion of axial bar and second term is related to equation of motion of beam bending, with moment of inertia equal to $A\ell_c^{g^2}$. In terms computational difficulty, nonlocal theory includes integral form of equation of motion and gradient theory includes fourth order differential equation for simple one dimensional example.*

Remark 3. *The conditions arrived through nonlocal theory gives only the details of Neumann boundary condition. Whereas, the virtual work approach made use in gradient theory provides information on both Dirichlet and Neumann boundary conditions. Wherein, higher order derivative of the displacement is related to nonstandard force and displacement fields. These higher order terms need to evaluated experimentally and uniquely defined at boundary. Such difficulties are avoided by comparing the Neumann boundary condition arrived in both the case. By comparing the eqs.34 and 64, a relation for double traction is obtained as*

$$T \;=\; \ell_c\, t \;-\; EA\ell_c\xi_1 \frac{du(L)}{dx} \tag{67}$$

6 Galerkin based weighted residual method

In the present work, we carry out numerical study of both integro-differential and gradient elasticity model. In this regard, we considered Galerkin based weighted residual approach to derive the matrix-vector form of the governing equation.

6.1 Integro-differential equation

The strong form of a nonlocal boundary value problem considering Dirichlet and Neumann type boundary conditions can be stated as follows: Find the displacement $\boldsymbol{u}(\boldsymbol{x}) : \Omega \mapsto \mathbb{R}^3$ such that the following equilibrium equation is satisfied.

$$\boldsymbol{\nabla} \cdot \boldsymbol{\sigma} + \boldsymbol{b} = 0 \quad \text{in} \quad \Omega \tag{68}$$

$$\text{given} \quad \boldsymbol{u} = \boldsymbol{u}_g \quad \text{on} \quad \Gamma_u \tag{69}$$

$$\boldsymbol{\sigma} \cdot \boldsymbol{n} = \boldsymbol{t} \quad \text{on} \quad \Gamma_t \tag{70}$$

$$\boldsymbol{\sigma}(\boldsymbol{x}) \;=\; \xi_1\, \boldsymbol{C} \;:\; \boldsymbol{\epsilon}(\boldsymbol{x}) \;+\; \xi_2 \int_{\mathrm{V}'} \alpha(\, \boldsymbol{x},\, \boldsymbol{x}',\, \ell_c\,)\, \boldsymbol{C} \;:\; \boldsymbol{\epsilon}(\boldsymbol{x}')\, d\mathrm{V}' \tag{71}$$

where $\boldsymbol{b}$ denotes body force. Consider a finite dimensional trial space $\mathfrak{S}^h$ and test space $\mathfrak{V}^h$ such that $\mathfrak{S}^h \subset \mathfrak{S}$ and $\mathfrak{V}^h \subset \mathfrak{V}$. Where $\mathfrak{S}$ and $\mathfrak{V}$ are the infinite dimension trial and test space. Then we can say

$$\mathfrak{S}^h \;=\; \{\, \boldsymbol{u}^h \in \mathcal{H}^1(\Omega) \mid \boldsymbol{u}^h = \boldsymbol{u}_g \;\text{ on }\; \Gamma_u \,\} \tag{72}$$

$$\mathfrak{V}^h \;=\; \{\, \boldsymbol{w}^h \in \mathcal{H}^1(\Omega) \mid \boldsymbol{w}^h = 0 \;\text{ on }\; \Gamma_u \,\} \tag{73}$$

where $\mathcal{H}^1(\Omega)$ is a Hilbert space controlling regularity of the trial and the test fields. The interest is to find a finite dimensional trial field, $\boldsymbol{u}^h \in \mathfrak{S}^h$, such that it holds for all choices of finite dimensional test function, $\boldsymbol{w}^h \in \mathfrak{V}^h$, following the integral equation

$$\int_\Omega \boldsymbol{\nabla} \boldsymbol{w}^h : \boldsymbol{\sigma} \; d\Omega = \int_\Omega \boldsymbol{w}^h \cdot \boldsymbol{b} \; d\Omega + \int_{\Gamma_t} \boldsymbol{w}^h \cdot \boldsymbol{t} \; d\Gamma_t \qquad \forall \; \boldsymbol{w}^h \in \mathfrak{V}^h \tag{74}$$

Including eq. 71 in eq. 74, the integral equation can written as

$$\xi_1 \int_\Omega \boldsymbol{\nabla} \boldsymbol{w}^h \; : \boldsymbol{C} : \; \boldsymbol{\epsilon} \; d\Omega \; + \; \xi_2 \int_\Omega \boldsymbol{\nabla} \boldsymbol{w}^h \; : \; \boldsymbol{C} \; : \left\{ \int_{\Omega'} \frac{1}{2l_c} \; e^{-\frac{|\boldsymbol{x}-\boldsymbol{x}'|}{l_c}} \, \boldsymbol{\epsilon}(\boldsymbol{x}') \; d\Omega' \right\} \; d\Omega =$$

$$\int_\Omega \boldsymbol{w}^h \cdot \boldsymbol{b} \; d\Omega \; + \int_{\Gamma_t} \boldsymbol{w}^h \cdot \boldsymbol{t} \; d\Gamma_t \qquad \forall \; \boldsymbol{w}^h \in \mathfrak{V}^h \tag{75}$$

Galerkin based weighted residual approach illustrate to discretize the global domain into elements and approximate the trial and test field variables over an each element.

$$\boldsymbol{u}_e^h = \boldsymbol{N}^e \boldsymbol{u}^e \quad \& \quad \boldsymbol{\nabla} \boldsymbol{u}_e^h = \boldsymbol{B}^e \boldsymbol{u}^e \tag{76}$$

$$\boldsymbol{w}_e^h = \boldsymbol{N}^e \boldsymbol{w}^e \quad \& \quad \boldsymbol{\nabla} \boldsymbol{w}_e^h = \boldsymbol{B}^e \boldsymbol{w}^e$$

Where $\boldsymbol{N}^e$ and $\boldsymbol{B}^e$ are the basis function and their derivative. The final form of integral equation after considering the divergence theorem and traction boundary condition is

$$\boldsymbol{w}^{e^T} \left\{ \xi_1 \int_{\Omega^e} \boldsymbol{B}^T(\boldsymbol{x}^e) \, \boldsymbol{C} \, \boldsymbol{B}(\boldsymbol{x}^e) \, d\Omega^e \; + \; \xi_2 \int_{\Omega^e} \sum^{N_{el'}} \int_{\Omega^{e'}} \boldsymbol{B}^T(\boldsymbol{x}^e) \, \boldsymbol{C} \, \frac{1}{2l_c} \, e^{\frac{-|\boldsymbol{x}^e - \boldsymbol{x}^{e'}|}{l_c}} \, \boldsymbol{B}(\boldsymbol{x}^{e'}) \; d\Omega^{e'} \; d\Omega^e \right\} \boldsymbol{u}^e$$

$$= \boldsymbol{w}^{e^T} \left\{ \int_{\Omega^e} \boldsymbol{N}^T(\boldsymbol{x}^e) \; \boldsymbol{b} \, d\Omega^e \; + \; \int_{\Gamma_t^e} \boldsymbol{N}^T(\boldsymbol{x}^e) \; \boldsymbol{t} \, d\Gamma_t^e \right\} \tag{77}$$

$$\boldsymbol{w}^{e^T} \left\{ \; \xi_1 \boldsymbol{K}_l^e + \xi_2 \boldsymbol{K}_{nl}^{ee'} \; \right\} \boldsymbol{u}^e = \boldsymbol{w}^{e^T} \boldsymbol{f}^e \qquad \forall \;\; \boldsymbol{w}^e \tag{78}$$

equation 78 is the matrix-vector form of the integral equation, where $\boldsymbol{K}_l^e$ and $\boldsymbol{K}_{nl}^{ee'}$ are the elemental stiffness matrix for the local and nonlocal case. The only difference observed with nonlocal stiffness is having extra spatial integral equation requiring an extra elemental looping in an computation scheme. At the end, matrix-vector form has to hold for all possible choices of $\boldsymbol{w}^e$ resulting force equilibrium equation as

$$\left\{ \; \xi_1 \, \boldsymbol{K}_l^e \; + \; \xi_2 \boldsymbol{K}_{nl}^{ee'} \; \right\} \boldsymbol{u}^e \; = \; \boldsymbol{f}^e \tag{79}$$

equation 79 is the discrete form equilibrium of forces obtained for each element and an assembly over each element results in global equation.

6.2 Mindlin simplified elasticity model

The strong form of a boundary value problem considering Dirichlet and Neumann boundary conditions are given in eqs. 62 to 66. Consider a finite dimensional trial space $\mathfrak{S}^h$ and test space $\mathfrak{V}^h$, given by

$$\mathfrak{S}^h = \left\{ u^h(x) \in \mathcal{H}_0^2(0,L) \;\middle|\; u^h = u_g \text{ on } \Gamma_u \quad \& \quad \frac{du^h}{dx} = \left(\frac{du}{dx}\right)_g \text{ on } \Gamma_u^* \right\} \tag{80}$$

$$\mathfrak{V}^h = \left\{ w^h(x) \in \mathcal{H}_0^2(0,L) \;\middle|\; w^h = 0 \text{ on } \Gamma_u \quad \& \quad \frac{dw^h}{dx} = 0 \text{ on } \Gamma_u^* \right\} \tag{81}$$

A strong requirement of C^1 continuity on trail and test field variables is ensured while choosing approximation. The integral equation can be written as

$$\int_0^L \left\{\frac{dw^h(x)}{dx}\right\} EA \left\{\frac{du^h(x)}{dx}\right\} dx + \int_0^L \frac{d^2w^h(x)}{dx^2} EA\ell_c^{g^2} \frac{d^2u^h(x)}{dx^2} dx = w^h(x)\Big|_{\Gamma_t} t + \frac{dw^h(x)}{dx}\Big|_{\Gamma_{t*}} T \tag{82}$$

In the next step, the trial and test fields are approximated over each element as given below

$$u_e^h(x) = \boldsymbol{N}^e \boldsymbol{u}^e, \qquad \frac{du_e^h(x)}{dx} = \boldsymbol{B}^e \boldsymbol{u}^e \quad \& \quad \frac{d^2u_e^h(x)}{dx^2} = \boldsymbol{C}^e \boldsymbol{u}^e \tag{83}$$

$$w_e^h(x) = \boldsymbol{N}^e \boldsymbol{w}^e, \qquad \frac{dw_e^h(x)}{dx} = \boldsymbol{B}^e \boldsymbol{w}^e \quad \& \quad \frac{d^2w_e^h(x)}{dx^2} = \boldsymbol{C}^e \boldsymbol{w}^e \tag{84}$$

Where, $\boldsymbol{N}^e$, $\boldsymbol{B}^e$ and $\boldsymbol{C}^e$ are the basis function, first and second derivatives of the basis function associated with test and trial filed variables. Including the eqs. 83 to 84 into eq. 82, the integral equation can be written as

$$\left\{ \int_{x_e}^{x_{e+1}} \boldsymbol{B}^{e^T} EA\, \boldsymbol{B}^e\, dx + \int_{x_e}^{x_{e+1}} \boldsymbol{C}^{e^T} EA\ell_c^{g^2}\, \boldsymbol{C}^e\, dx \right\} \boldsymbol{u}^e = \left\{ \boldsymbol{N}^{e^T}\Big|_{\Gamma_t} t + \boldsymbol{B}^{e^T}\Big|_{\Gamma_{t*}} T \right\} \tag{85}$$

By making use of eq. 67 to replace the double traction, the integral equation is written as

$$\left\{ \int_{x_e}^{x_{e+1}} \boldsymbol{B}^{e^T} EA\, \boldsymbol{B}^e\, dx + \int_{x_e}^{x_{e+1}} \boldsymbol{C}^{e^T} EA\ell_c^{g^2}\, \boldsymbol{C}^e\, dx + \int_{\Gamma_{t*}} \boldsymbol{B}^{e^T} EA\ell_c\xi_1\, \boldsymbol{B}^e\, dx \right\} \boldsymbol{u}^e = \left\{ \boldsymbol{N}^{e^T}\Big|_{\Gamma_t} + \boldsymbol{B}^{e^T}\Big|_{\Gamma_{t*}} \ell_c \right\} t \tag{86}$$

$$\left\{\boldsymbol{K}^e + \boldsymbol{K}_*^e + \boldsymbol{K}_*^{\Gamma^e}\right\} \boldsymbol{u}^e \;=\; \boldsymbol{f}^e \tag{87}$$

The explicit presence of double traction is completely removed and the term $K_*^{\Gamma^e}$ included in domain integration. A careful measure is taken to evaluate $K_*^{\Gamma^e}$ only at boundary points. Further, the external force, $\boldsymbol{f}^e$, is modified accordingly.

7 Numerical Examples

In order to explore the capabilities of integro-differential and gradient elasticity theory in predicting the size effect, a simple one dimensional example is considered. Further, the effect of considering higher order and higher continuity approximation in terms of computation effort is also made. In this regard, three different approximations: Lagrangian basis, Bèzier basis and B-spline basis, are considered for the analysis. The purpose of the study is to see how each approximation is able to capture the size effect with $h-$ and $p-$ refinements. Which of the basis is computationally expensive. In the end comparisons of both theories are made.

7.1 Integro-differential model

A tensile bar fixed on left end and subjected to an axial force at the right end is considered for the analysis, see Fig. **??**. The model parameters considered are: modulus of elasticity is $E = 200\,\text{GPa}$, cross sectional area is $A = 10\,\text{mm}^2$ and the length of the bar is $L = 100\,\text{mm}$. The point force at the right free end of the bar is taken as $F = 100\,\text{N}$. The length scale and nonlocal parameter is taken equal to $\ell_c = 0.01\,L$ and $\xi_1 = 2$, see [36, 48] for more information.

In traditional case the band width of global stiffness matrix is related to the influence domain of approximation. Whereas in nonlocal theories such matrix is enriched. In the sense the support length of Kernel function increases the band width of matrix. For example, if the support length of Kernel function is taken equal to finite element size then the traditional stiffness matrix is recovered. As Kernel values on neighbor element is zero. In this regard, the minimum size of finite element is taken less than the support length of Kernel function.

Fig. **??** illustrates plot of normalized strain versus position along longitudinal direction obtained for Lagrange approximation. Further, an increase in order of polynomial from linear to quintic, i.e. $p-$ refinement, and increase in degrees of freedom from 25 to 100 degrees of freedom, i.e. $h-$ refinement, are explored. Lagrangian approximation predicts the size effect for both cases of $h-$ refinement and $p-$ refinement. But the limitations are (i) C^0 based finite element method requiring a larger number of nodes to predict size effect resulting

computational approach expensive and (ii) oscillations in the solution is associated with C^0 continuity at inter element boundary.

Bèzier basis posses better continuity within the element than Lagrangian as they be-

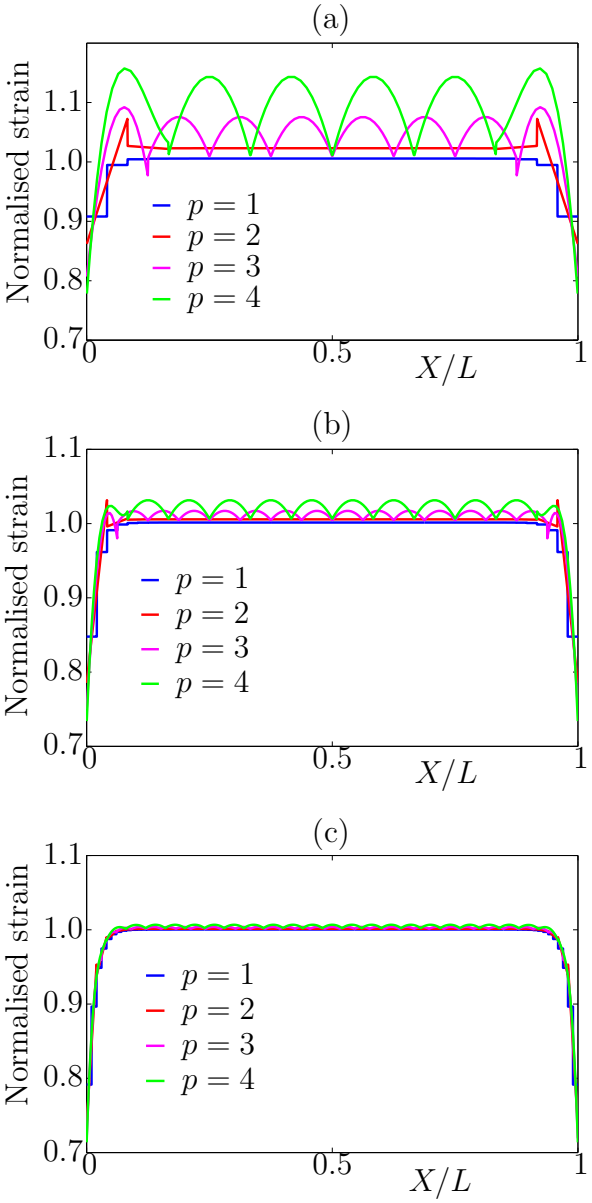

Figure 6: Lagrangian approximation results for: (a) 25 Dof (b) 50 Dof and (c) 100 Dof

long to family of splines. Moreover, the basis are point-wise positive and do not satisfy the Kronecker delta property at interior control points. However there is no much change is observed in predicting the size effect, see Fig. **??**. Thus, clearly indicating that to predict the size effect, one way is to improve the continuity at the inter element boundary.

Fig. **??** illustrate the $p-$ and $h-$ refinement results for the case of B-spline approximation. This shows that the size effect is predicted for higher continuity approximation and proves to be computationally less expensive. In the sense, an increase in the inter-element continuity results in the following changes (i) increase in the global number of elements for fixed global number of nodes and (ii) an increase in the size of overlapping element stiffness matrix. For example, let NN, NE and p be the global number of nodes, global number of elements and order of polynomial. Then, the NE required for C^0 approximation is (NN-1)/p and for C^{p-1} approximation is NN-p. Thus, an higher continuity approximation result in increased NE for given NN. Further, the size of global stiffness matrix is fixed to size NNxNN. Then for higher continuity approximation, the increased elements is accommodated by increasing the size of overlapping element stiffness matrix. Which can be treated as a non-locality introduced through numerical approach. In that way the global stiffness matrix is further enriched along with nonlocal theory. Which allowed to predict the size effect correctly and with less computational effort.

7.2 Gradient elasticity model

In the next case, a gradient elasticity results will be explored for one dimensional example and also compared with nonlocal results. The input parameter considered earlier is retained for present case also. The other parameter need to be evaluated is length scale and it is given by $\ell_c^g = \ell_c\sqrt{\xi_1}$. In terms of implementation point view, the difficulty is associated with generating higher order approximation and finding higher derivative of approximation. Unlike spending large amount of time in evaluating the double integration in the case of nonlocal theory. Moreover, the study also includes exploring effect higher order and higher continuity approximation on computational time.

Fig. **??** illustrates plot of normalized strain versus position along longitudinal direction obtained for Lagrange approximation. Further $p-$ refinement, order varying form 3 to 11, and $h-$ refinement, dofs varying from 25 to 100, results are explored. These figures depicts that the gradient theory predicts the size effect and therefore they can act as replacement for nonlocal theories. A similar results are observed for Bèzier approximation, see Fig. **??**. Comparing the nonlocal and gradient results, the oscillation of the solution is absent with latter case. The reason is associated with governing equation derived seeking for both dis-

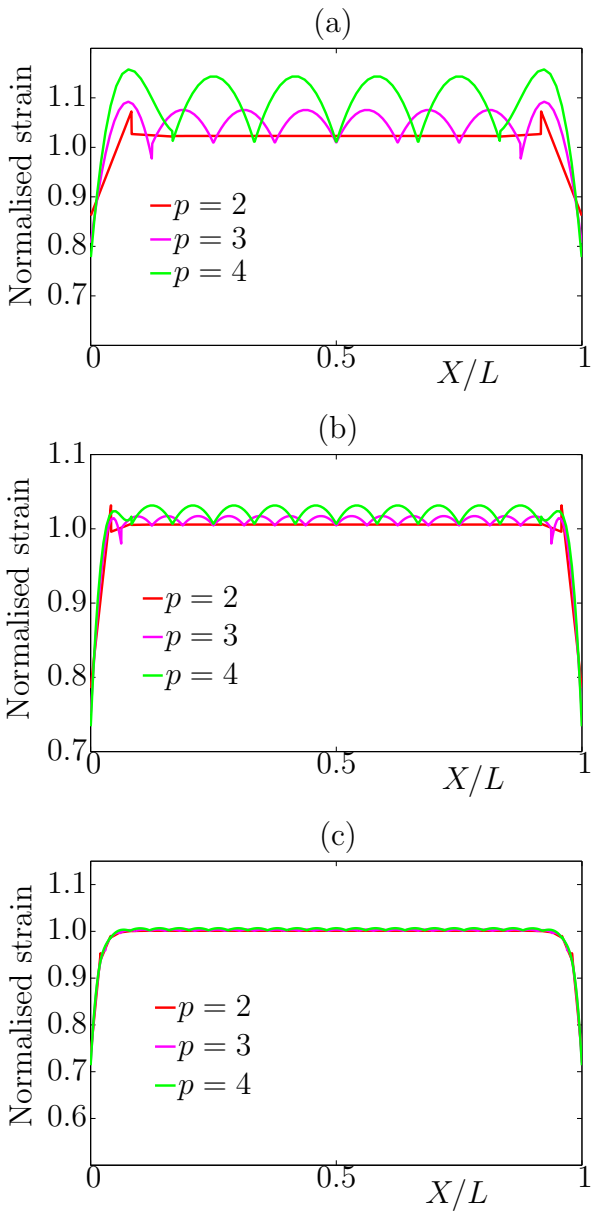

Figure 7: Bèzier approximation results for: (a) 25 Dof (b) 50 Dof and (c) 100 Dof

placement and derivative of the displacement be very smooth function.

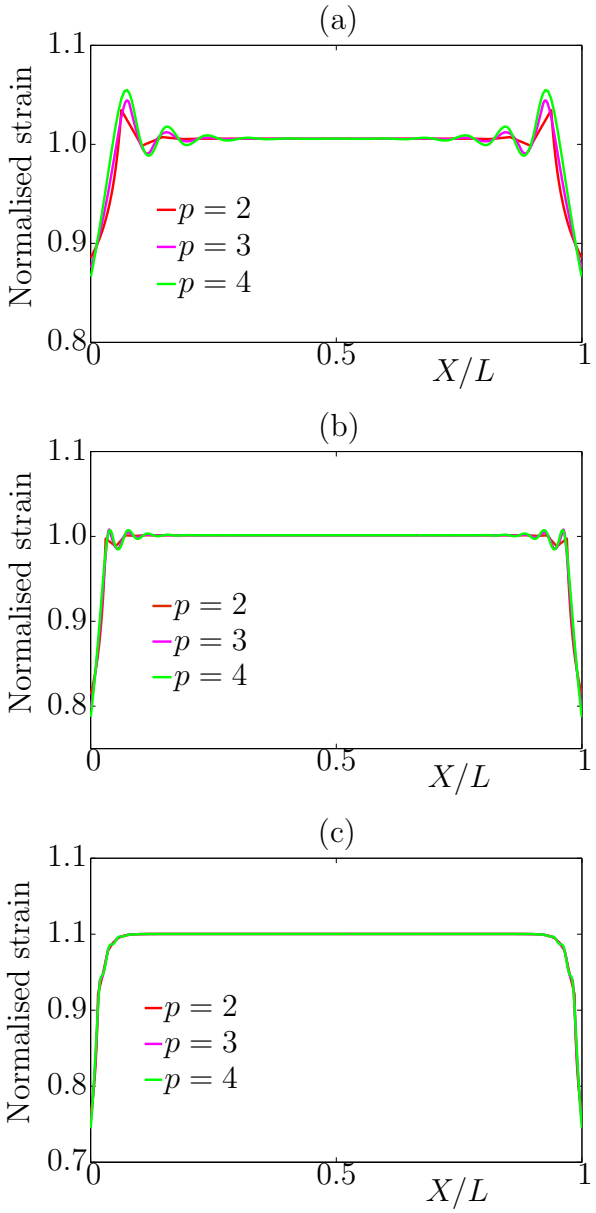

Figure 8: B-spline approximation results for: (a) 25 Dof (b) 50 Dof and (c) 100 Dof

In the next case the gradient elasticity results are explored by improving the continuity of approximation through B-spline. The $p-$ refinement, order varying form 4 to 20, and $h-$ refinement, dofs varying from 25 to 100, results are obtained as shown in Fig. **??**. Comparing

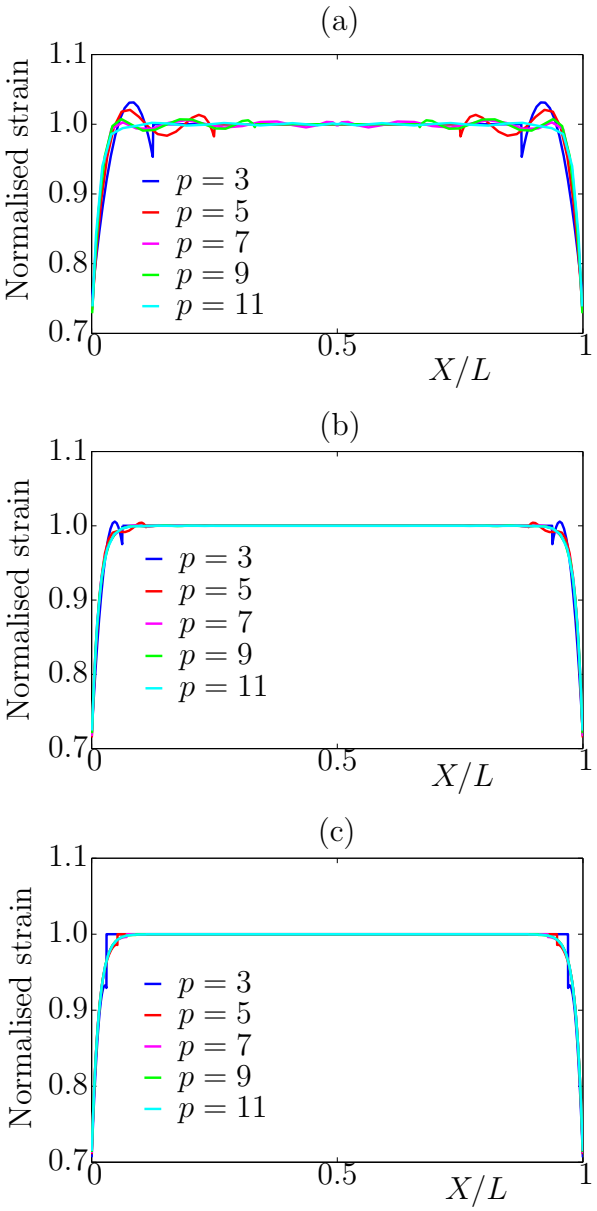

Figure 9: Lagrangian approximation results for: (a) 25 Dof (b) 50 Dof and (c) 100 Dof

the Figs. **??** and **??** following conclusions are made

1. A very large order of approximation is required to predict the size effect for the case of B-spline than the Lagrange approximation. The issue is associated with boundary

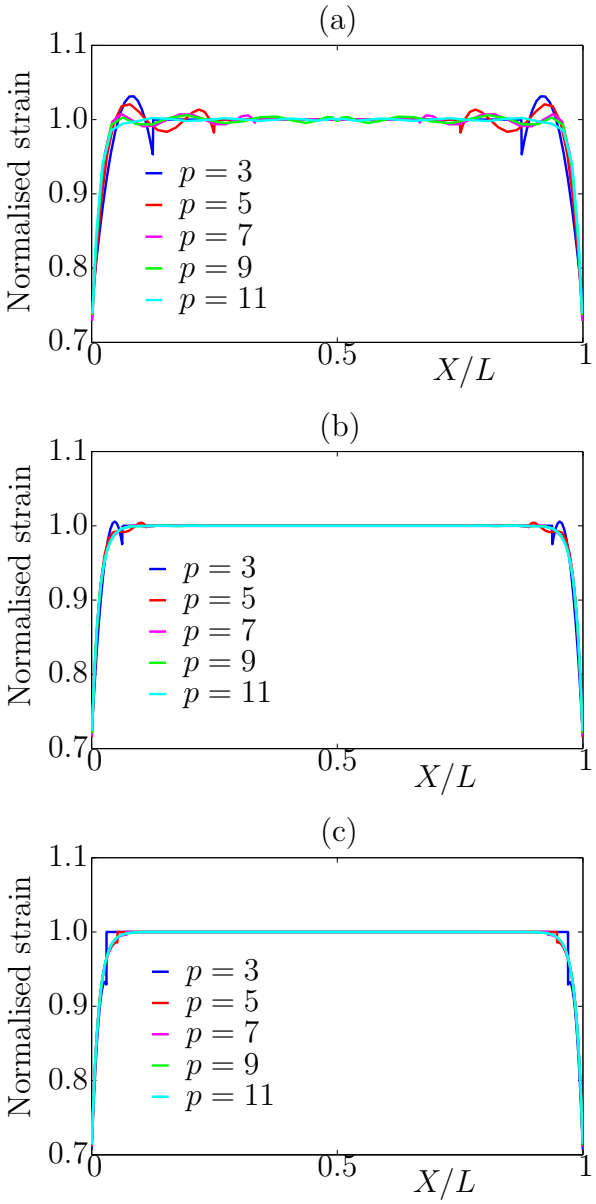

Figure 10: Bèzier approximation results for: (a) 25 Dof (b) 50 Dof and (c) 100 Dof

oscillation which are completely absent for Lagrange approximation. Therefore, considering higher continuity approximation proves computational expensive than Lagrange approximation.

2. Moreover, in the case of nonlocal theories oscillation is observed for Lagrange approximation than higher continuity approximation. But a reverse case is seen for gradient elasticity model.

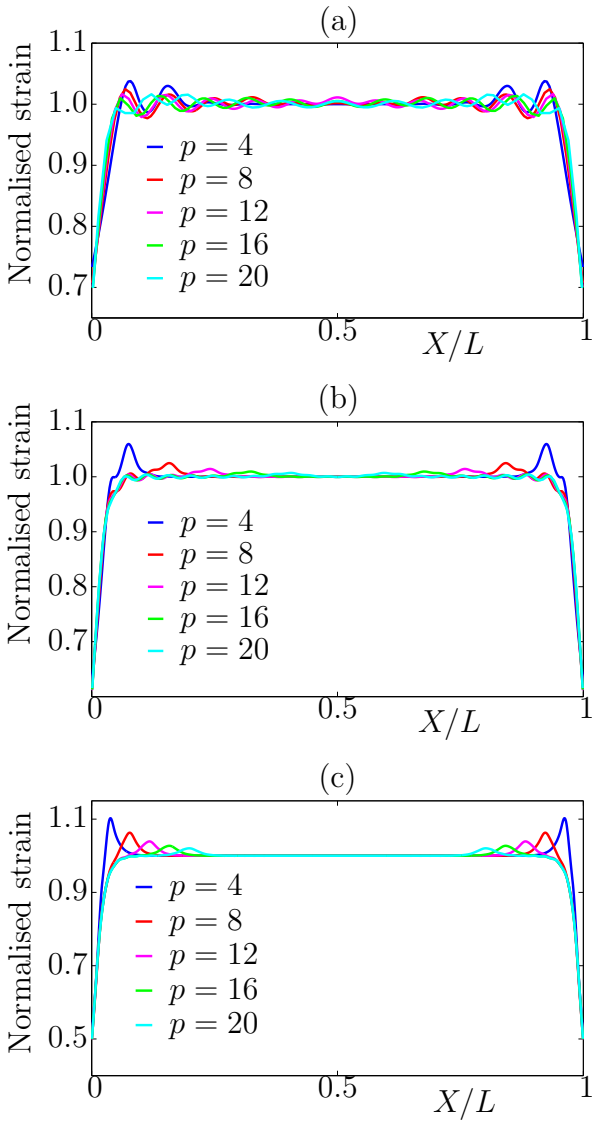

Figure 11: B-spline approximation results for: (a) 25 Dof (b) 50 Dof and (c) 100 Dof

8 Conclusion

In the present work the nonlocal-differential form of integro-differential equation and Mindlin higher order gradient elasticity model is reviewed for the case of one-dimensional example. The difficulties associated with higher order model is the experimental evaluation of material length scale and higher order boundary conditions. But the similarity exist between the nonlocal differential form and gradient elasticity model provide solution in such case. In the sense that a relation is derived between length scales, i.e. ℓ_c and ℓ_c^g, and the traction boundary conditions, i.e. t and T. In terms implementation, both nonlocal-differential form and gradient elasticity models are considered to predict the size effect of one-dimensional example. Further we considered higher order and higher continuity approximations for the study. In the first case of nonlocal differential model, C^0 continuous approximation proves to be computationally expensive. The setback of such approach is, C^0 continuity at inter-element boundary. Which introduces the oscillation in the solution and requiring very large element discretization. Whereas higher continuity approximation proves to be less expensive. In second case of gradient elasticity model, higher continuity approximation proves to be computationally expensive. As boundary oscillation will be present and vanishes for very large order of approximation. whereas, C^0 continuous approximation proves to be less expensive. The conclusion is, higher continuous approximation are best suited for integral form of governing equation and higher order approximation is best suited for differential form of governing equation.

References

[1] R. D. Mindlin and H. F. Tiersten. Effects of couple stresses in linear elasticity. *Archive for Rational Mechanics and Analysis*, 11:415–448, 1962.

[2] R. D. Mindlin. Microstructure in linear elasticity. *Archive for Rational Mechanics and Analysis*, 16:51–78, 1964.

[3] A. C. Eringen. Simple microfluids. *International Journal of Engineering Science*, 2:205–2178, 1964.

[4] A. E. Green and R. S. Rivlin. Multipolar continuum mechanics. *Archive for Rational Mechanics and Analysis*, 17:113–147, 1964.

[5] A. E. Green. Micromaterials and multipolar continuum mechanics. *International Journal of Engineering Science*, 3:533–537, 1965.

[6] E. S. Rajagopal. The existence of interfacial couples in infinitesimal elasticity. *Ann. Phys. (Leipzig)*, 6:192–201, 1960.

[7] C. Truesdell and R. A. Toupin. *Classical field theories of mechanics*. Springer, Berlin, 1960.

[8] E. Cosserat and R. Cosserat. *Theorie des corps deformables*. Herman, Paris, 1909.

[9] E. Kröner. Elasticity theory of materials with long range cohesive forces. *International Journal of Solids and Structures*, 3:731–742, 1967.

[10] I. A. Kunin. The theory of elastic media with microstructure and the theory of dislocations, mechanics of generalized continua. *In: E. Kroner, ed., Springer, Heidelberg*, pages 321–329, 1968.

[11] J. A. Krumhansl. *Some consideration on the relations between solid state physics and generalized continuum mechanics*. 1968.

[12] A. C. Eringen. Line crack subjected to shear. *International Journal of Fracture*, 14:367–379, 1978.

[13] A. C. Eringen. Line crack subjected to anti-plane shear. *Engineering Fracture Mechanics*, 12:211–219, 1979.

[14] A. C. Eringen and B. S. Kim. Stress concentration at the tip of a crack. *Mechanics Research Communications*, 1:233–237, 1974.

[15] A. C. Eringen, C. G. Speziale, and B. S. Kim. Crack-tip problem in non-local elasticity. *Journal of the Mechanics and Physics of Solids*, 25:339–355, 1977.

[16] A. C. Eringen. On differential equations of nonlocal elasticity and solutions of screw dislocation and surface waves. *Journal of Applied Physics*, 54:4703–4710, 1983.

[17] A. C. Eringen. Theory of nonlocal elasticity and some applications. *Res Mechanica*, 21(4):313–342, 1987.

[18] Q. S. Nguyen. *A thermodynamic description of the running crack problem*. In: S. Neemat-Nasser (Ed.), Three-dimensional constitutive relations and ductile fracture, North-Holland, Amsterdam, 1980.

[19] C. Zang and B. L. Karihaloo. A thermodynamic framework of fracture mechanics. *Engineering Fracture Mechanics*, 46:1023–1030, 1993.

[20] A. C. Eringen. On nonlocal plasticity. *International Journal Engineering Science*, 2:1461–1474, 1981.

[21] A. C. Eringen. Theories of nonlocal plasticity. *International Journal Engineering Science*, 21:741–751, 1983.

[22] C. Polizzotto. Thermodynamics and continuum fracture mechanics for nonlocal-elastic plastic materials. *European Journal of Mechanics A/Solids*, 21:85–103, 2002.

[23] C. Polizzotto. A nonlocal strain gradient plasticity theory for finite deformations. *International Journal of Plasticity*, 25:1280–1300, 2009.

[24] M. Jirasek. Nonlocal models for damage and fracture: comparison of approaches. *International Journal of Solids and Structures*, 35:4133–4145, 1998.

[25] Z. P. Bazant and M. Jirasek. Nonlocal integral formulations of plasticity and damage: Survey and progress. *Journal of Engineering Mechanics ASCE*, 128(5-6):1119–1149, 2002.

[26] E. Benvenuti, G. Borino, and A. Tralli. A thermodynamically consistent nonlocal formulation for damaging materials. *European Journal of Mechanics A/Solids*, 21:535–553, 2002.

[27] D. Rogula. Introduction to nonlocal theory of material media. *Journal of the Mechanics and Physics of Solids*, 25:339–355, 1977.

[28] S. B. Altan. Uniqueness of the initial-value problems in nonlocal elastic solids. *International Journal of Solids and Structures*, 25:1271–1278, 1989.

[29] S. B. Altan. Existence in nonlocal elasticity. *Archive Mechanics*, 41:25–36, 1989.

[30] C. Polizzotto. Nonlocal elasticity and related variational principles. *Journal of Solids and Structures*, 38:7359–7380, 2001.

[31] J. N. Reddy. Nonlocal theories for bending, buckling and vibration of beams. *International Journal of Engineering Science*, 45:288–307, 2007.

[32] M. Aydogdu. Axial vibration of the nanorods with the nonlocal continuum rod model. *Physica E*, 41:861–864, 2009.

[33] S. Adhikari, T. Murmu, and M. A. McCarthy. Frequency domain analysis of nonlocal rods embedded in an elastic medium. *Physica E*, 59:33–40, 2014.

[34] O. Civalek and C. Demir. Bending analysis of microtubules using nonlocal euler-bernoulli beam theory. *Applied Mathematical Modelling*, 35:2053–2067, 2011.

[35] A. A. Pisano and P. Fuschi. Closed form solution for a nonlocal elastic bar in tension. *International Journal of Solids and Structures*, 40:13–23, 2003.

[36] E. Benvenuti and A. Simone. One-dimensional nonlocal and gradient elasticity: Closed form solution and size effect. *Mechanics Research Communications*, 48:46–51, 2013.

[37] H. Askes and E. C. Aifantis. Gradient elasticity in statics and dynamics: An overview of formulations, length scale identification procedures, finite element implementations and new results. *International Journal of Solids and Structures*, 48:1962–1990, 2011.

[38] D. J. Bammann and E. C. Aifantis. On a proposal for a continuum with microstructure. *Acta Mechanica*, 45:91–121, 1982.

[39] D. Walgraef and E. C. Aifantis. Dislocation patterning in fatigued metals as a result of dynamical instabilities. *Journal of Applied Physics*, 58:688–691, 1985.

[40] E. C. Aifantis. On the microstructural origin of certain inelastic models. *Journal of Engineering Materials and Technology (Trans. ASME)*, 106:326–330, 1984.

[41] E. C. Aifantis. On the role of gradients in the localization of deformation and fracture. *International Journal of Engineering Science*, 30:1279–1299, 1992.

[42] E. C. Aifantis. Pattern formation in plasticity. *International Journal of Engineering Science*, 33:2161–2178, 1995.

[43] N. A. Fleck, G. M. Müller, M. F. Ashby, and J. W. Hutchinson. Strain gradient plasticity: Theory and experiment. *Acta Metallurgica et Materialia*, 42:475–487, 1994.

[44] H. Gao, Y. Huang, W. D. Nix, and J. W. Hutchinson. Mechanism-based strain gradient plasticity i. theory. *Journal of the Mechanics and Physics of Solids*, 47:1239–1263, 1999.

[45] S. B. Altan and E. C. Aifantis. On the structure of the mode iii crack-tip in gradient elasticity. *Scripta Metallurgica et Materialia*, 26(2):319–324, 1992.

[46] C. Q. Ru and E. C. Aifantis. A simple approach to solve boundary-value problems in gradient elasticity. *Acta Mechanica*, 101(1):59–68, 1993.

[47] K. R. Rajagopal and A. R. Srinivasa. On a class of non-dissipative materials that are not hyperelastic. *Proceedings of the Royal Society of London A*, 465:493–500, 2009.

[48] M. Malagù, E. Benvenuti, C. A. Duarte, and A. Simone. One-dimensional nonlocal and gradient elasticity: Assessment of high order approximation schemes. *Computer methods in applied mechanics and engineering*, 275:138–158, 2014.

[49] L. Piegl and W. Tiller. *The NURBS Book (Monographs in Visual Communication)*. (Second ed.)Springer-Verlag, New York, 1997.

[50] A. C. Eringen. Linear theory of nonlocal elasticity and dispersion of plane waves. *International Journal of Engineering Science*, 10(5):425–435, 1972.

[51] J. N. Reddy. *An introduction of continuum mechanics*. Cambridge University Press, New York, NY, 2013.

[52] A. D. Polianin and A. V. Manzhirov. *Handbook of integral equations*. CRC Press,, 2008.

[53] J. Peddieson, G. R. Buchanan, and R. P. McNitt. Application of nonlocal continuum models to nanotechnology. *International Journal of Engineering Science*, 41:305–312, 2003.

[54] N. Challamel and C. M. Wang. The small length scale effect for a non-local cantilever beam: A paradox solved. *Nanotechnology*, 19:1–10, 2008.

[55] J. Sulem and I. G. Vardoulakis. *Bifurcation analysis in geomechanics*. CRC Press, 2004.

Appendix A Deriving the boundary conditions

In order derive the boundary condition for differential form of integro-differential equation, we recall the eq. 29 once again and write in more compact form as follows

$$\epsilon(x) \;=\; \frac{\xi_1}{\xi_2}\left[\mathcal{S}(x) \;-\; \ell_c^2\,\frac{d^2\mathcal{S}(x)}{dx^2}\right] \tag{88}$$

Where,

$$\mathcal{S}(x) \;=\; \frac{\bar{\epsilon}}{\xi_1} \;-\; \epsilon(x) \tag{89}$$

Including the eq. 88 in to nonlocal strain eq. 24 results

$$\epsilon_{nl}(x) \;=\; \frac{\xi_1}{\xi_2}\mathcal{S}_{nl}(x) \;-\; \frac{\xi_1\,\ell_c^2}{\xi_2}\int_0^L \alpha(x,x',\ell_c)\,\frac{d^2\mathcal{S}(x')}{dx'^2}\,dx' \tag{90}$$

The chosen Kernel function, eq. **??**, is a symmetric and discontinuous function at point x. Thus, it is possible to split the function into two parts at x. Accordingly, the integration also split into two integrals.

$$\alpha(x, x', \ell_c) = \begin{cases} \frac{1}{2\,\ell_c}\, e^{-(x-x')/\ell_c} & \text{for} \quad x \geq x' \\ \frac{1}{2\,\ell_c}\, e^{-(x'-x)/\ell_c} & \text{for} \quad x' \geq x \end{cases} \tag{91}$$

$$\epsilon_{nl}(x) \;=\; \frac{\xi_1}{\xi_2}\mathcal{S}_{nl}(x) \;-\; \frac{\xi_1\,\ell_c^2}{\xi_2}\left[\;\int_0^x \alpha(x, x', \ell_c)\,\frac{d^2\mathcal{S}(x')}{dx'^2}\,dx' \;+\; \int_x^L \alpha(x, x', \ell_c)\,\frac{d^2\mathcal{S}(x')}{dx'^2}\,dx'\right] \tag{92}$$

Using the rule of integration, i.e. the domain integration is divided into domain and boundary part, the above equation is simplified as follows

$$\epsilon_{nl}(x) \;=\; \frac{\xi_1}{\xi_2}\,\mathcal{S}_{nl}(x) \;-\; \frac{\xi_1\,\ell_c^2}{\xi_2}\left[\alpha(x, x', \ell_c)\,\frac{d\mathcal{S}(x')}{dx'}\bigg|_{x'=0}^{x'=x} \;-\; \frac{d\alpha(x, x', \ell_c)}{dx'}\;\mathcal{S}(x')\bigg|_{x'=0}^{x'=x} \;+\right.$$

$$\int_0^x \frac{d^2\alpha(x, x', \ell_c)}{dx'^2}\,S(x')\;dx' \;+\; \alpha(x, x', \ell_c)\,\frac{d\mathcal{S}(x')}{dx'}\bigg|_{x'=x}^{x'=L} \;-\; \frac{d\alpha(x, x', \ell_c)}{dx'}\;\mathcal{S}(x')\bigg|_{x'=x}^{x'=L} \;+$$

$$\left.\int_x^L \frac{d^2\alpha(x, x', \ell_c)}{dx'^2}\,\mathcal{S}(x')\;dx'\right] \tag{93}$$

The first and second derivative of the Kernel function are as given below

$$\frac{d\alpha(x, x', \ell_c)}{dx'} = \begin{cases} \frac{1}{2\,\ell_c^2}\, e^{-(x-x')/\ell_c} & \text{for} \quad x \geq x' \\ -\frac{1}{2\,\ell_c^2}\, e^{-(x'-x)/\ell_c} & \text{for} \quad x' \geq x \end{cases} \tag{94}$$

$$\frac{d^2\alpha(x, x', \ell_c)}{dx'^2} \;=\; \frac{1}{2\,\ell_c^3}\, e^{-|x-x'|/\ell_c} \quad \forall \quad x' \tag{95}$$

Making use of eqs. 94 to 95 into eq. 93 results

$$\epsilon_{nl}(x) \;=\; -\,\frac{\xi_1\,\ell_c^2}{\xi_2}\left[\alpha(x, x', \ell_c)\,\frac{d\mathcal{S}(x')}{dx}\bigg|_{x'=0}^{x'=x} \;-\; \frac{1}{\ell_c}\,\alpha(x, x', \ell_c)\;\mathcal{S}(x')\bigg|_{x'=0}^{x'=x} \;+\right.$$

$$\left.\alpha(x, x', \ell_c)\,\frac{d\mathcal{S}(x')}{dx}\bigg|_{x'=x}^{x'=L} \;+\; \frac{1}{\ell_c}\,\alpha(x, x', \ell_c)\;\mathcal{S}(x')\bigg|_{x'=x}^{x'=L}\right] \tag{96}$$

Another interesting property of Kernel function is the Dirac delta value at $x' = x$.

$$\text{i.e.} \quad \alpha(x, x, \ell_c) = \delta(x, x, \ell_c) = 1 \tag{97}$$

Making use of Dirac delta value and applying the integrand values, the equation is further simplified as

$$\epsilon_{nl}(x) = \frac{\xi_1}{\xi_2}\mathcal{S}(x) + \frac{\ell_c}{2}\frac{\xi_1}{\xi_2}\left[\alpha(x,0,\ell_c)\left\{\frac{d\mathcal{S}(0)}{dx} - \frac{1}{\ell_c}\mathcal{S}(0)\right\} - \alpha(x,L,\ell_c)\left\{\frac{d\mathcal{S}(L)}{dx} + \frac{1}{\ell_c}\mathcal{S}(L)\right\}\right] \tag{98}$$

Using eq. 89 the final form can be written as

$$\xi_1\,\epsilon(x) + \xi_2\,\epsilon_{nl}(x) = \bar{\epsilon} + \frac{\ell_c\,\xi_1}{2}\left[\alpha(x,0,\ell_c)\left\{\frac{d\mathcal{S}(0)}{dx} - \frac{1}{\ell_c}\mathcal{S}(0)\right\} - \alpha(x,L,\ell_c)\left\{\frac{d\mathcal{S}(L)}{dx} + \frac{1}{\ell_c}\mathcal{S}(L)\right\}\right] \tag{99}$$

The eq. 99 looks similar to eq. 25 excluding the presence of second term in right hand side. In order retain the similarity between those equations, the condition arrived are

$$\frac{d\mathcal{S}(0)}{dx} - \frac{1}{\ell_c}\mathcal{S}(0) = 0 \tag{100}$$

$$\frac{d\mathcal{S}(L)}{dx} + \frac{1}{\ell_c}\mathcal{S}(L) = 0 \tag{101}$$

Expressing in terms of strain results

$$\frac{d\epsilon(0)}{dx} - \frac{\epsilon(0)}{\ell_c} = -\frac{1}{\ell_c\,\xi_1}\,\bar{\epsilon} \tag{102}$$

$$\frac{d\epsilon(L)}{dx} + \frac{\epsilon(L)}{\ell_c} = \frac{1}{\ell_c\,\xi_1}\,\bar{\epsilon} \tag{103}$$